Carcinogenesis, 2015, Vol. 36, No. 11, 1363–1371

doi:10.1093/carcin/bgv106
Advance Access publication August 11, 2015
Original Manuscript

ORIGINAL MANUSCRIPT

miR-544a induces epithelial–mesenchymal transition through the activation of WNT signaling pathway in gastric cancer

Yoshimitsu Yanaka[1,2], Tomoki Muramatsu[1], Hiroyuki Uetake[2], Ken-ichi Kozaki[1,3,4] and Johji Inazawa[1,3,5,*]

[1]Department of Molecular Cytogenetics, Medical Research Institute, [2]Department of Surgical Oncology and [3]Bioresource Research Center, Graduate School, Tokyo Medical and Dental University, 1-5-45 Yushima, Bunkyo-ku, Tokyo 113-8510, Japan, [4]Department of Dental Pharmacology, Okayama University Graduate School of Medicine, Dentistry and Pharmaceutical Sciences, Okayama University, Okayama 700-8525, Japan and [5]Hard Tissue Genome Research Center, Graduate School, Tokyo Medical and Dental University, Tokyo 113-8510, Japan

*To whom correspondence should be addressed. Tel: +81 3 5803 5820; Fax: +81 3 5803 0244; Email: johinaz.cgen@mri.tmd.ac.jp

Abstract

The epithelial–mesenchymal transition (EMT) contributes to cancer progression, as well as the development of normal organs, wound healing and organ fibrosis. We established a cell-based reporter system for identifying EMT-inducing microRNAs (miRNAs) with a gastric cancer (GC) cell line, MKN1, transfected with a reporter construct containing a promoter sequence of *VIM* in the 5′ upstream region of the TurboRFP reporter gene. Function-based screening using this reporter system was performed with a 328-miRNA library, and resulted in the identification *miR-544a* as an EMT-inducing miRNA. Although *miR-544a* is already known to be involved in the regulation of *CDH1*, the mechanism by which EMT occurs remains poorly understood. Herein, we demonstrated that overexpression of *miR-544a* induces *VIM*, *SNAI1* and *ZEB1* expression, and reduces *CDH1* expression, resulting in an EMT phenotype. In addition, we found that *CDH1* and *AXIN2*, which are related to the degradation and the translocation of β-catenin, are direct targets of *miR-544a*. Subsequently, the reduction of *CDH1* and *AXIN2* by *miR-544a* induced the nuclear import of β-catenin, suggesting that *miR-544a* may activate the WNT signaling pathway through the stabilization of β-catenin in nucleus. Our findings raise the possibility that inhibition of *miR-544a* may be a therapeutic target of metastatic GC.

Introduction

Gastric cancer (GC) results in a considerable amount of morbidity and mortality, and the incidence of GC is the fifth most common malignancy worldwide. Seventy percent of these cases occur in developing countries, among which half occurs in East Asia (1). In Japan, GC was the second leading cause of cancer-related death in 2013 (2). Clinically, it has recently become possible to cure GC completely if detected early. However, the prognosis of metastasized GC still remains poor in contrast to that of early GC.

Recently, there is growing interest focused around understanding the role of the epithelial–mesenchymal transition (EMT) in cancer progression (3,4). It is known that EMT contributes to increasing migration, invasion and metastasis in cancer, and also is involved in embryogenesis in normal tissue (5,6). When EMT is stimulated, cell–cell adhesion and cell polarity are disrupted by disappearance of adhesion molecules such as E-cadherin, resulting in the acquisition of a mesenchymal phenotype. Consequently, cells which have acquired mesenchymal function activate the migratory and invasion capability in cancer (7). For example, activation of the TGF pathway suppresses expression of E-cadherin and the *microRNA-200* family, and maintains the mesenchymal phenotype through several

Received: February 11, 2015; **Revised:** July 15, 2015; **Accepted:** July 17, 2015

Abbreviations

EMT	epithelial–mesenchymal transition
GC	gastric cancer
LEF	lymphoid enhancer factor
miRNA	microRNA
qRT-PCR	quantitative RT-PCR
TCF	T-cell factor
UTR	untranslated region

EMT-related transcription factors such as TWIST, and those of the ZEB family and SNAI family (3–9). However, details of the EMT regulatory network remain unclear.

MicroRNAs (miRNAs) are endogenous small non-coding, single-stranded RNAs of approximately 22 nucleotides that suppress gene expression post-transcriptionally by binding to complementary sites within the 3′ untranslated region (3′ UTR) of their mRNA targets (10). miRNAs play important roles in maintaining homeostasis in the body pertaining to processes involved in development, differentiation, proliferation and apoptosis (11). Additionally, miRNAs can function as tumor suppressor and oncogenes in cancer (12–14). Related to the regulation of EMT, miRNAs have been identified in several studies, especially the *miR-200* family which inhibits EMT through suppression of the *ZEB* family genes (15). Recently, *miR-655* has also been identified as a novel EMT-suppressive miRNA by using the *CDH1* reporter screening system (16). In contrast, few EMT-inducing miRNAs have been identified. These EMT regulatory miRNAs might be important diagnostic markers and aid in the development of new therapeutic agents for human malignancies.

In this current study, we identified a novel EMT-inducing miRNA by function-based screening of 328 synthetic miRNAs and characterized their function including examination of direct targets. The function-based screening can evaluate the biological effects of a large number of miRNAs on cancer cells directly. Additionally, this approach has already been demonstrated as useful in the exploration of miRNAs in their oncogenic or tumor suppressive effects on cancer cells (16–19). Using our cell-based reporter system, we previously identified *miR-655* as being involved in the expression of GFP through dependence on the *CDH1* promoter activity (16). In this study, we established a novel cell-based reporter system, in which expression of TurboRFP is dependent on the *VIM* promoter activity in a GC cell line, MKN1, having phenotypic plasticity for EMT/mesenchymal–epithelial transition. We identified *miR-544a* as an EMT-inducing miRNA and showed that *miR-544a* directly regulates both *CDH1* (E-cadherin) and *AXIN2*, resulting in the induction of the nuclear import of β-catenin; in other words, *miR-544a* induces EMT through activation of the WNT signaling pathway. Our findings suggest a potential role for *miR-544a* as a therapeutic target for metastatic GC.

Materials and methods

Cell lines

Characteristics and sources of the 29 GC cell lines used in the present study are listed in Supplementary Table S1, available at *Carcinogenesis* Online. GC cell lines were authenticated in our previous studies of array-CGH analyses (20). All cells except for AGS cells were cultured in RPMI 1640 (Gibco, Grand Island, NY) supplemented with 10% fetal bovine serum; AGS cells were cultured in Ham's F12. Total RNA and protein were extracted from each cell line as described elsewhere (21).

Western blotting and immunofluorescent staining

The following primary antibodies were used for western blotting or immunofluorescent staining: anti-E-Cadherin (#610181), anti-β-Catenin (#610153) (BD Biosciences, Franklin Lakes, NJ), anti-TCF8/ZEB1 (#3396), anti-APC2 (#12301), anti-GSK3β (#9315) (Cell Signaling Technology, Danvers, MA), anti-Vimentin Ab-2 (Clone V9, Thermo Fisher Scientific, Waltham, MA), anti-AXIN2 (ab109307) (abcam, Cambridge, UK), anti-tRFP (AB233) (Evrogen, Moscow), anti-β-actin, anti-β-tubulin (Sigma, St. Louis, MO) and anti-Lamin B (C-20) (sc-6216, Santa Cruz Biotechnology, Santa Cruz, CA). Western blotting and immunofluorescent staining were performed as described elsewhere (16). The cytoplasmic and nuclear fractions were prepared with the NE-PER extraction kit (Thermo Scientific) according to the manufacturer's instructions.

Quantitative real-time RT-PCR

Total RNA was extracted using TRIzol reagent (Invitrogen, Carlsbad, CA) according to standard procedures. Single-stranded cDNA generated from the total RNA was amplified with a primer set specific for each gene. The quantitative RT-PCR (qRT-PCR) was performed using the KAPA SYBR system (Kapa Biosystems, Wilmington, MA) and an ABI PRISM 7500 sequence detection System (Applied Biosystems, Foster City, CA) according to the manufacturer's instructions.

Gene expression values are expressed as ratios between genes of interest and an internal reference gene (glyceraldehyde-3-phosphate dehydrogenase, GAPDH), and subsequently normalized with the value for the control (relative expression level). For miRNAs, qRT-PCR was performed using an ABI Prism 7500 Fast Real-time PCR System, Taqman Universal PCR Master Mix, Taqman Reverse Transcription kit and Taqman MicroRNA Assays (Applied Biosystems), according to the manufacturer's instructions. Expression levels of miRNA genes were based on the amount of the target message relative to that of the *RNU6B* transcript as a control to normalize the initial input total RNA (22). All samples were analyzed in a duplicated manner.

Luciferase activity assay

Luciferase reporter plasmids were made by inserting the 3′-UTR of *CDH1*, *AXIN2* and *APC2* downstream of the luciferase gene within pmirGLO Dual-Luciferase miRNA Target Expression Vector (Promega, Madison, WI). All site-specific mutations were using the GeneTailor site-directed mutagenesis system (Invitrogen). Luciferase reporter plasmids and pTK plasmids as the internal control were cotransfected in MKN1 cells or MKN28 cells, and the *miR-544a* or negative control-miRNA was transfected 5 h later. After 2 or 3 days, Firefly and Renilla luciferase activities were measured using the Dual-Luciferase Reporter Assay System (Promega), and relative luciferase activity was calculated by normalizing the Firefly luciferase reading with its corresponding internal Renilla luciferase control (16).

TCF/LEF reporter assay

We purchased the Cignal T-cell factor (TCF)/lymphoid enhancer factor (LEF) Reporter (luc) Kit (CS-018L) from QIAGEN. According to the manufacture's instruction, Cignal Reporter or Cignal Negative Control as the internal control and *miR-544a* or negative control were cotransfected in MKN28 cells, and medium was changed 24 h later. After 3 days, Firefly and Renilla luciferase activities were measured using the Dual-Luciferase Reporter Assay System (Promega), and relative luciferase activity was calculated by normalizing the Firefly luciferase reading with its corresponding internal Renilla luciferase control (15).

Transfection with synthetic miRNAs

A total of 10 nmol/l of miRNA was transfected individually into cells using Lipofectamine RNAiMAX (Invitrogen) according to manufacturer's instructions. The dsRNA mimicking human mature miRNA for *miR-504-5p* (PM12429, *miR-544a* (PM12414), *let-7c-5p* (PM10436), *miR-105-5p* (PM12838), *miR-107* (PM10056), *miR-126-3p* (PM12841), *miR-9-5p* (PM10022), *miR-29a-3p* (PM12499), *miR-29b-3p* (PM10103), *miR-103a-3p* (PM10632), *miR-200a-3p* (PM10991), *miR-200b-3p* (PM10492), *miR-200c-3p* (PM11714), *miR-655-3p*(PM11619) and negative control #1 were purchased from Ambion. All the overexpression experiments of each miRNA was performed transiently.

Plasmid construction and transfection

The promoter region of *VIM* (23) was obtained by PCR and inserted into a promoterless expression vector, pTurboRFP-PRL vector (Evrogen). The generated construct was verified by sequencing. The plasmid DNA was transfected into MKN1 cells using Lipofectamine 2000 (Invitrogen) according to the manufacturer's instructions.

Cell survival assay

The numbers of viable cells were assessed by the crystal violet staining assay. The cells were washed in phosphate-buffered saline and fixed with 0.2% crystal violet in 10% formaldehyde in phosphate-buffered saline for 5 min. Excess crystal violet solution was discarded, and after being completely air-dried, the stained cells were lysed with a 2% SDS solution by shaking the plates for 1 h. Optical density absorbance was measured at 560 nm using a microplate reader (ARVOmx; PerkinElmer, Waltham, MA), and the percent absorbance of every well was determined. The optical density absorbance values of cells in control wells were arbitrarily set at 100% to determine the percentage of viable cells.

Screening system using a promoterless expression vector, pTurboRFP-PRL

The stable clone, PVimRFP-MKN1 cells, was established by the limiting dilution method after transfection of the reporter construct into MKN1 cells. First, PVimRFP-MKN1 (2.5×10^4 cells per well) was seeded on 24-well plates. After 24 h, 10 nmol/l of each of 328 miRNA from Pre-miRTM miRNA Precursor Library-Human V2 (Ambion) or negative control-miRNA was transfected in duplicate manner. After 72 h, the fluorescence intensity of the TurboRFP protein was measured by ARVO mx (Perkin Elmer). At the

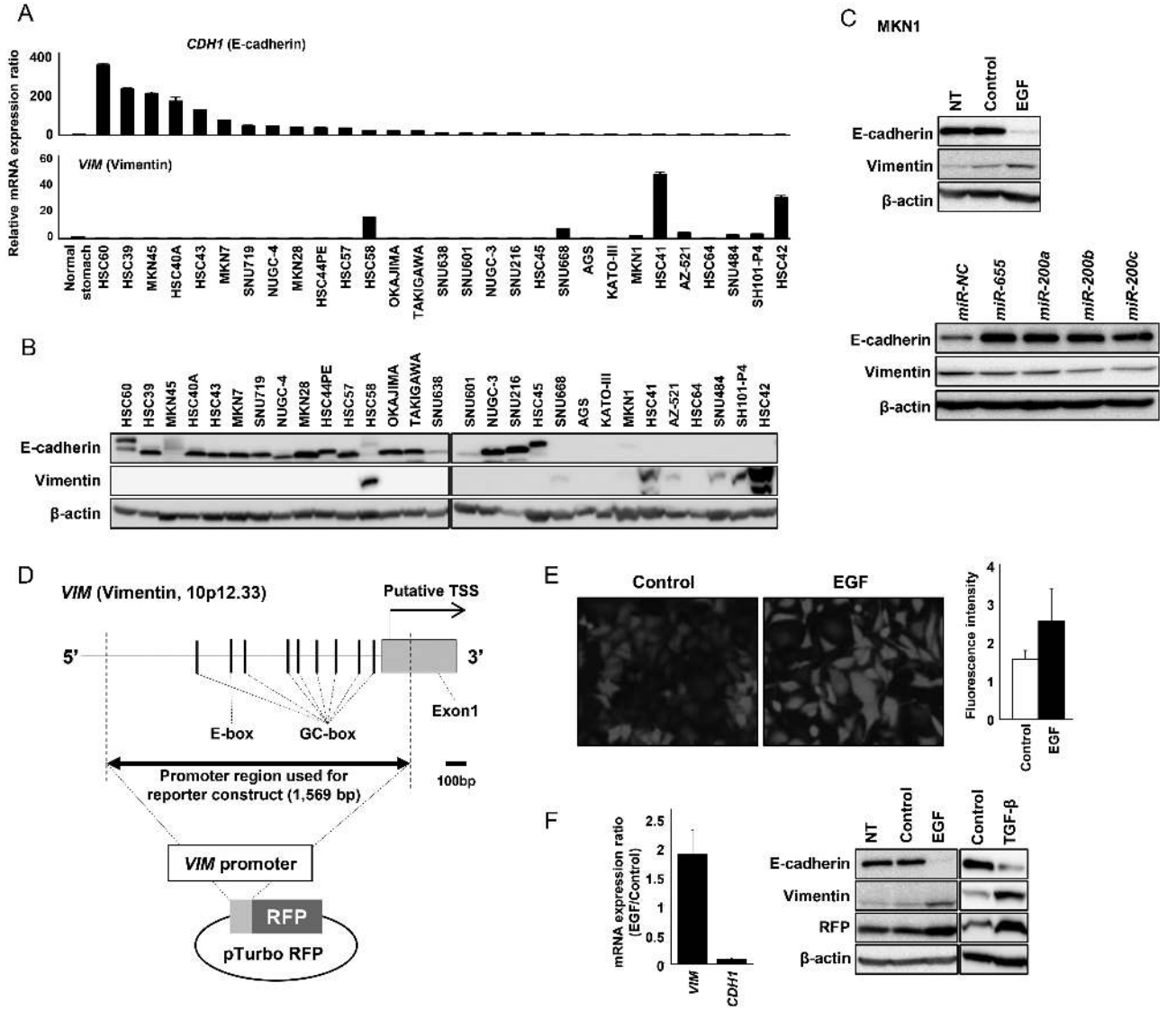

Figure 1. Establishment of a cell-based reporter system for identifying EMT-inducing miRNAs. (**A**, **B**) EMT status of 29 GC cell lines. (A) qRT-PCR and (B) western blotting were performed to examine the expression of *CDH1* (E-cadherin) and *VIM* (Vimentin) in these cell lines. The results were arranged based on *CDH1* mRNA expression with the highest levels beginning on the left. (**C**) MKN1 cells were incubated with 50 ng/ml EGF (upper) and transfected with *miR-200a,b,c* and -655 (bottom) for 72 h. E-cadherin and Vimentin expression were analyzed by western blotting. (**D**) Map of the promoter region of the *VIM* gene. Promoter sequences of the *VIM* gene (1569 bp) are indicated by the closed arrow in this map and were inserted into a promoterless pTurboRFP-PRL vector with the TurboRFP gene as a reporter gene. A cell-based reporter system was established by isolating a stable clone with the limiting dilation method after transfection of this construct into MKN1 cells. (**E**) Confirmation of TurboRFP protein expression in this system following treatment of 50 ng/ml EGF. A stable cell clone with the reporter plasmid was evaluated 72 h after treatment of 50 ng/ml EGF, or control (PBS). TurboRFP expression was observation in these transfectants using a fluorescent microscope. Fluorescence intensity was quantification in these transfectants. (**F**) Results of the TaqMan qRT-PCR analysis for expression of *VIM* and *CDH1* transcript (left). Results of the western blot analysis for expression of Vimentin and E-cadherin and TurboRFP protein with treatment of 50 ng/ml EGF, 25 ng/ml TGF-β (right) or control.

same time, living cells were enumerated by the crystal violet staining assay. The relative fluorescence intensity was calculated by the formula, the fluorescence intensity/the living cell rate.

Statistical analysis

Differences between subgroups were tested with the Mann–Whitney *U* test.

Results

The MKN1 GC cell line has plasticity of EMT

To investigate EMT status of 29 GC cell lines, we examined the expression of *CDH1* (E-cadherin) and *VIM* (vimentin) in these cell lines by qRT-PCR and western blotting. We observed that the expression of vimentin was inversely correlated with expression of E-cadherin in mRNA and at the protein level (Figure 1A and B), and we classified EMT phenotype in these cell lines based on EMT status. Then, we focused on MKN1 which expressed E-cadherin and vimentin, and investigated whether this cell line has the plasticity of EMT by treatment of EGF or transfection of miRNAs such as the *miR-200* family. EMT of MKN1 cells were induced (induction of vimentin expression, reduction of E-cadherin expression) by treatment with 50 ng/ml EGF, whereas overexpression of *miR-200a*, *b*, *c* and -655 showed mesenchymal–epithelial transition phenotype (induction of E-cadherin expression, reduction of vimentin expression) in this cell (Figure 1C). These results suggested that MKN1 cells have the plasticity of EMT; thus, we applied it to a cell-based reporter system for investigating *VIM*-promoter activity with MKN1 cells.

Establishment of a cell-based reporter system for investigating *VIM*-promoter activity with MKN1 cells

To conduct function-based screening of EMT-inducing miRNAs, we established a cell-based reporter system. The promoter region of the *VIM* gene (23) located in the 5′ untranslated region (5′ UTR) and exon 1 (from nt −1497 to +89 relative to the transcription start site, TSS, at the 5′ end of the gene) was prepared by genomic PCR using specific primers, and was inserted into the promoterless expression vector, pTurboRFP-PRL, at the multiple cloning site upstream of the TurboRFP gene (PVimRFP) (Figure 1D). We first transfected the PVimRFP into MKN1 cells, and then carried out cloning of stable transfectants by limiting dilution. Then, we selected a single clone (PVimRFP-MKN1) which was most sensitive to EGF and TGF-β, cytokines known to be EMT-inducing. In PVimRFP-MKN1, the fluorescence intensity and protein level of TurboRFP were remarkably increased by treatment with 50 ng/ml EGF or 25 ng/ml TGF-β compared with control, and we observed the induction of vimentin expression

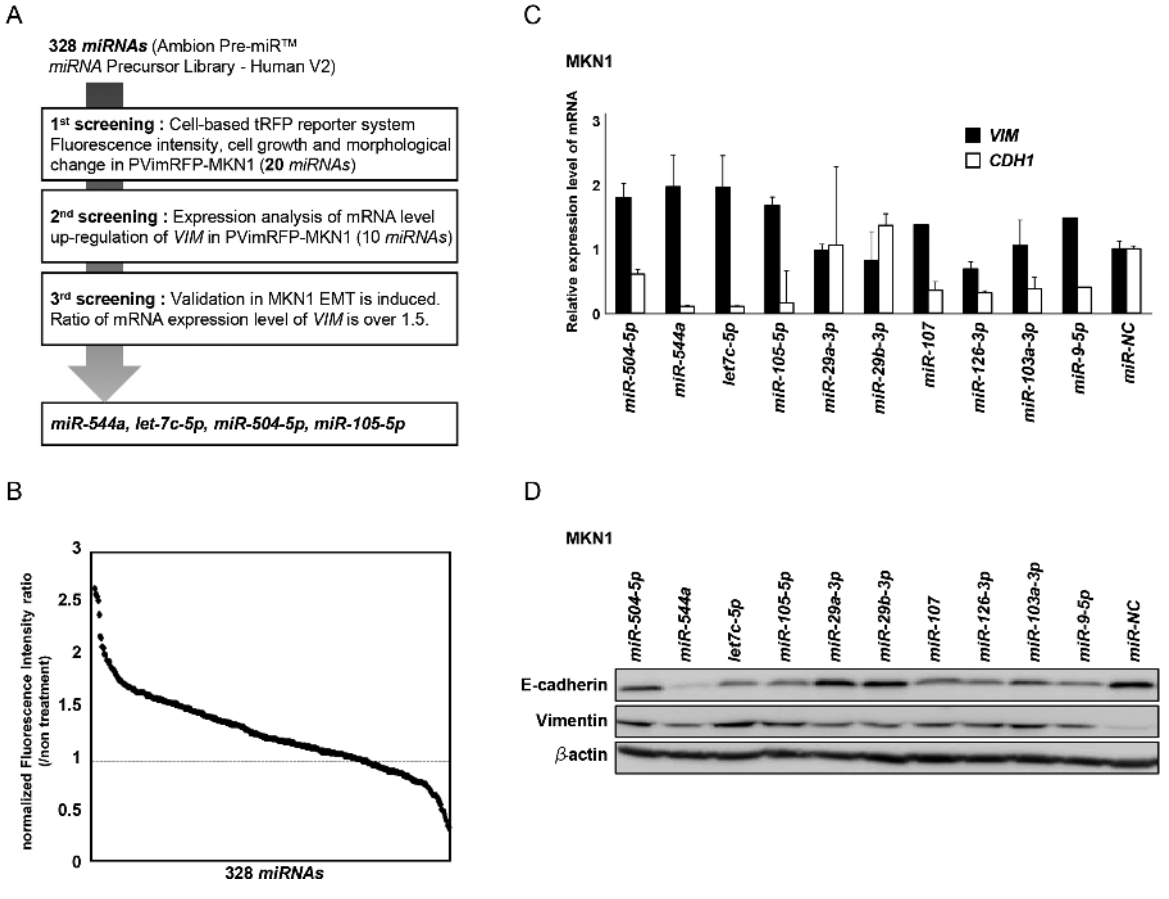

Figure 2. The function-based screening of EMT-inducing miRNAs using the cell-based VIM reporter system in MKN1 cells. (**A**) The screening chart of this study. (**B**) Result of first screening using Pre-miRTM miRNA Precursor Library-Human V2 (Ambion) containing 328 dsRNAs mimicking human mature miRNAs. The fluorescence intensity of TurboRFP was evaluated by the fluorescence microplate reader in duplicate. The relative fluorescence intensity in each transfectant was calculated to the fluorescence intensity in control cells (non-treatment) and normalized by cell number measured by the crystal violet method (Supplementary Table 2, available at *Carcinogenesis* Online). (**C**, **D**) Evaluation of Vimentin and E-cadherin expression in MKN1, transfected with each candidate miRNA selected in the second screening. (C) Results of TaqMan qRT-PCR analysis for expression of *VIM* and *CDH1* in MKN1 cells. The value is an average of the three experiments. (D) Results of the western blot analysis of Vimentin and E-cadherin protein levels in MKN1 cells for 72 h after transient transfection with 10 nM of *miR-NC*, *-9-5p*, *-29a-3p*, *-29b-3p*, *-103a-3p*, *-105-5p*, *-107*, *-126-3p*, *-504-5p*, *-544a* and *let-7c-5p*.

and reduction of E-cadherin expression (Figure 1E and F). These results suggested that the expression of TurboRFP and vimentin were synchronized. Thus, we concluded that TurboRFP expression was tightly regulated under the *VIM*-promoter in our cell-based reporter system for function-based screening of EMT-inducing miRNAs.

Function-based screening of EMT-inductive miRNAs with our cell-based reporter system

To identify EMT-inducing miRNAs, we performed function-based screening, in which the fluorescence intensity of TurboRFP was made into an own manner, using our cell-based reporter system and 328 dsRNAs at 10 nM. The strategy and partial results are shown in Figure 2A. Figure 2B shows results of this screening in PVimRFP-MKN1 72 h after transfection with each miRNA (Supplementary Table 2, available at *Carcinogenesis* Online). In Table 1, 20 miRNAs were considered candidate EMT-inducing miRNAs. Among them, 15 miRNAs satisfied the following criteria; (i) the relative fluorescence intensity that markedly increased (1.5-fold change of mean fluorescence intensity compared with the control), (ii) no influence on cell growth (the normalized optical density absorbance value is between 0.5 and 1.5). Furthermore, we selected five miRNAs which produced a markedly altered cell shape into a form similar to mesenchymal cells. This resulted in the selection of 10 miRNAs (*miR-9-5p, -29a-3p*, *-29b-3p*, *-103a-3p*, *-105-5p*, *-107*, *-126-3p*,*-504-5p*, *-544a* and *let-7c-5p*) as EMT-inducing candidate miRNAs. To validate whether these candidate miRNAs induce EMT, we performed qRT-PCR after transfection of each miRNA in MKN1 cells. Overexpression of four miRNAs induced expression of *VIM* and a reduced expression of *CDH1* compared with control (Figure 2C). Furthermore, we confirmed the protein expression of vimentin and E-cadherin in MKN1 cells (Figure 2D), and found that overexpression of *miR-544a* significantly reduced the expression of E-cadherin compared with control, suggesting *miR-544a* to be a prime candidate as an EMT-inducing miRNA.

miR-544a promotes cell motility and invasion *in vitro* through EMT phenotype change

To determine whether *miR-544a* induces EMT phenotype, we checked expression of other EMT markers in MKN1 and MKN28 cell lines. Expression of Snail, an EMT-inducing transcriptional factor, was increased by *miR-544a* in MKN1 and MKN28. In addition, expression of ZEB1 was also induced by *miR-544a* in MKN1 (Figure 3A and B). These results suggested that EMT by miR-544a was induced through Snail and ZEB1. We next performed migration and invasion assay for revealing EMT function by *miR-544a*. Then, we confirmed that overexpression of *miR-544a* did not altered the cell growth compared with *miR-negative control* (*miR-NC*) in MKN1 and MKN28 cell lines (Figure 3C). Cell motility and invasion abilities were investigated in *miR-NC* and *miR-544a* transfectants by transwell migration and invasion assay *in vitro*. *miR-544a* overexpressed cells showed faster cell migration and invasion through matrigel-coated or uncoated membranes, respectively, than the *miR-NC*-transfectant in MKN1 and MKN28 cell lines (Figure 3D and E). These results showed that *miR-544a* induced EMT through the typical pathway such as Snail and ZEB1.

Table 1. Summary of 20 miRNA genes selected as candidates for EMT-induced miRNAs in functional-based screening using a stable MKN1 clone transfected with a reporter construct containing a promoter sequence of *VIM* in the upstream region of the RFP reporter gene and Pre-miRTM miRNA Precursor Library—Human V2 (Ambion)

	Pre-miR™ miRNA Precursor	Mature sequence	Ratio of fluorescence intensity of TurboRFP (RFI)[a]		Ratio of growth level (RG)[b]		Relative fluorescence intensity (RFI/RG)		Morphology change
			Mean	SD	Mean	SD	Mean	SD	
1	hsa-miR-489-3p	AGUGACAUCACAUAUACGGCAGC	0.498	0.070	0.199	0.066	2.586	0.506	++
2	hsa-miR-544a	AUUCUGCAUUUUUAGCAAGU	1.205	0.013	0.556	0.008	2.168	0.056	–
3	hsa-miR-9-5p	UCUUUGGUUAUCUAGCUGUAUGA	0.816	0.024	0.421	0.029	1.937	0.078	++
4	hsa-miR-103a-3p	AGCAGCAUUGUACAGGGCUAUGA	0.982	0.096	0.511	0.093	1.935	0.162	–
5	hsa-miR-29a-3p	UAGCACCAUCUGAAAUCGGUU	1.001	0.008	0.530	0.032	1.890	0.098	–
6	hsa-miR-504-5p	AGACCCUGGUCUGCACUCUAU	0.734	0.028	0.392	0.045	1.882	0.143	++
7	hsa-miR-514a-3p	AUUGACACUUCUGUGAGUAG	0.983	0.049	0.542	0.100	1.851	0.431	–
8	hsa-miR-380-3p	UAUGUAAUAUGGUCCACAUCUU	1.144	0.027	0.653	0.012	1.754	0.074	–
9	hsa-miR-126-3p	UCGUACCGUGAGUAAUAAUGC	1.013	0.035	0.577	0.024	1.754	0.013	–
10	hsa-miR-29b-3p	UAGCACCAUUUGAAAUCAGUGUU	0.954	0.050	0.554	0.031	1.722	0.006	–
11	hsa-miR-296-5p	AGGGCCCCCCCUCAAUCCUGU	0.943	0.015	0.552	0.008	1.709	0.002	–
12	hsa-miR-523-3p	AACGCGCUUCCCUAUAGAGGG	0.944	0.001	0.555	0.009	1.702	0.029	+
13	hsa-miR-517a-3p, hsa-miR-517b-3p	AUCGUGCAUCCCUUUAGAGUGUU	0.677	0.023	0.398	0.008	1.698	0.024	++
14	hsa-miR-30b-5p	UGUAAACAUCCUACACUCAGCU	0.880	0.033	0.543	0.094	1.650	0.346	–
15	hsa-let-7c-5p	UGAGGUAGUAGGUUGUAUGGUU	0.935	0.078	0.576	0.128	1.650	0.231	–
16	hsa-let-7d-5p	AGAGGUAGUAGGUUGCAUAGU	1.013	0.033	0.617	0.045	1.644	0.067	–
17	hsa-miR-107	AGCAGCAUUGUACAGGGCUAUCA	1.039	0.023	0.640	0.019	1.622	0.011	–
18	hsa-miR-154-5p	UAGGUUAUCCGUGUUGCCUUCG	0.859	0.007	0.545	0.119	1.617	0.368	+
19	hsa-miR-105-5p	UCAAAUGCUCAGACUCCUGU	0.682	0.069	0.422	0.016	1.613	0.103	++
20	hsa-miR-30a-5p	UGUAAACAUCCUCGACUGGAAG	0.928	0.048	0.589	0.074	1.584	0.116	–

[a]The ratio of fluorescence intensity of RFP (RFI) in cells 72 h after transfection with each miRNA was normalized to that in control transfectants (Pre miRTM Negative Control #1, Ambion).

[b]The ratio of growth level (RG) of viable cells assessed by crystal violet staining 72 h after transfection with miRNAs. This assay was employed to normalize the number of viable cells relative to the control transfectants.

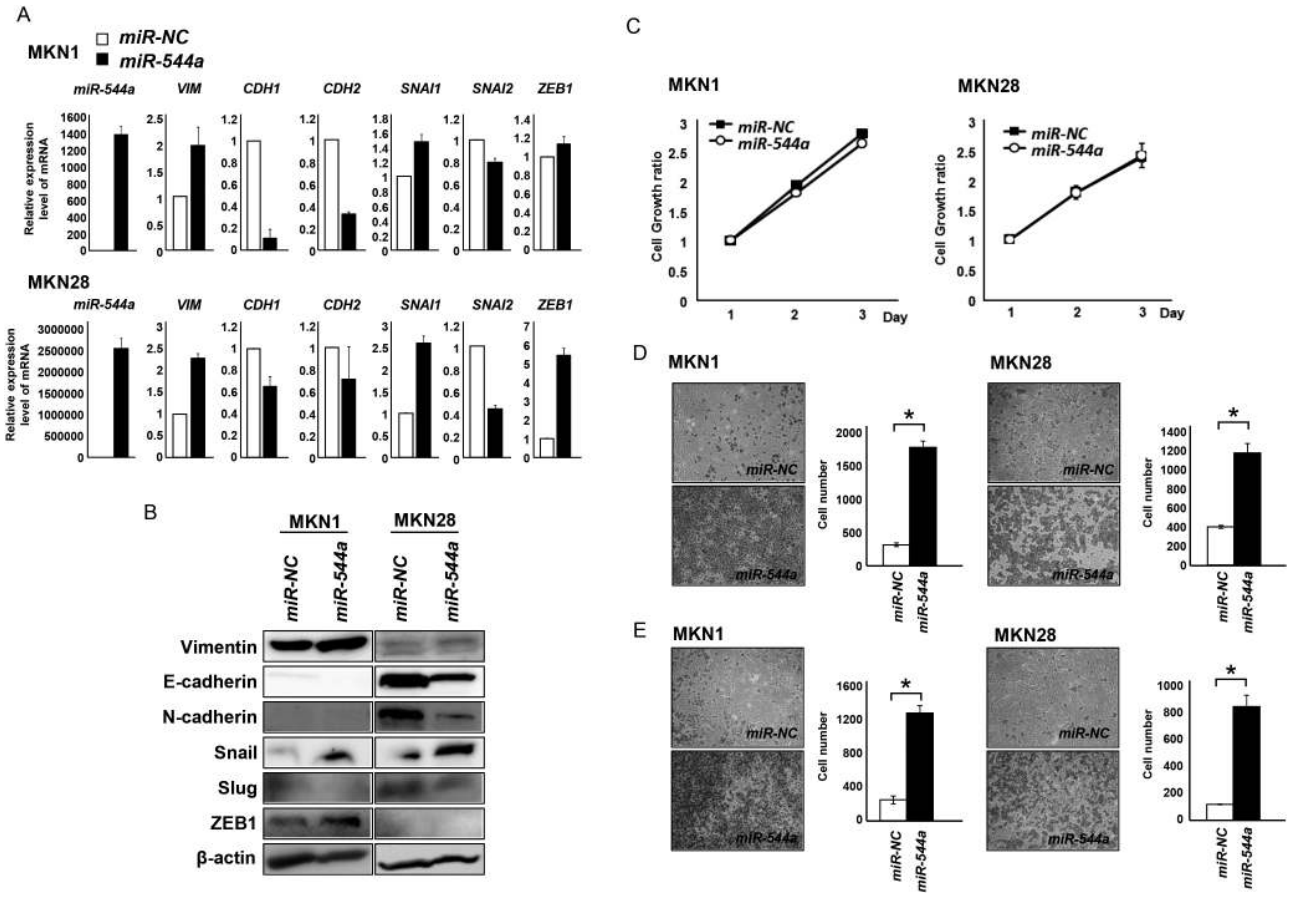

Figure 3. *miR-544a* promotes cell motility and invasion through EMT phenotype change. (**A**, **B**) Expression of EMT markers in *mRNA* and protein levels was confirmed by qRT-PCR (A), with mean ± SD (bars) of duplicate experiments, or by western blotting (B) in MKN1 and MKN28 cell lines, 72 h after transfection of *miR-544a*. (**C**) The number of viable cells 24–72 h after transfection of *miR-544a* (5 nM) and *miR-NC* (5 nM) was assessed by WST-8 assay. Each data point represents the mean of quadruplicate experiments (bars, SD). (**D**, **E**) Transwell migration and invasion assays were carried out in 24-well modified Boyden chambers without and with matrigel (BD transduction), respectively. Cells [2×10^4 cells per well (migration assay) or 4×10^4 cells per well (invasion assay)] were transferred into the upper chamber, and the migrated or invaded cells on the lower surface of the filters were fixed, stained and counted after 36 h of incubation. Experiments were performed in triplicate, and each data point represents the mean (bars, SD). The Mann–Whitney *U*-test was used for statistical analysis; asterisks represent $P < 0.05$ versus each control transfectant.

miR-544a induces EMT by regulating nuclear import of β-catenin

To investigate other EMT-inducing mechanisms of *miR-544a*, we first focused on *CDH1*, which is known to be a direct target of *miR-544a*. Since we observed that reduced expression of E-cadherin correlates with overexpression of *miR-544a*, we examined whether *miR-544a* directly targets *CDH1* which has two predicted regions for binding of *miR-544a* in the 3′ UTR. We performed the luciferase reporter assay using vectors containing the wild-type or mutant of each region of the 3′UTR in *CDH1*. We detected statistically significant reductions in luciferase activity in wild-type constructs and not in mutant constructs in region 2, whereas *miR-544a* could not bind to region 1 (Figure 4A), indicating that *CDH1*was a direct target of *miR-544a*. Next, we hypothesized that β-catenin translocates from the cytoplasm to the nucleus through the reduction of E-cadherin by *miR-544a*. It is already known that β-catenin maintains the cell-cell contact through the cadherin–catenin complex and is a key regulator in the canonical WNT signaling pathway. β-catenin in the nucleus functions as an activator for TCF/LEF transcription factors that result in the induction of EMT. To evaluate whether this hypothesis is correct, we performed immunofluorescence analysis and western blotting using the cytoplasm or the nucleus separated samples in MKN28 cells. We observed that β-catenin translocated from the cytoplasm to the nucleus by overexpression of *miR-544a* in both analyses (Figure 4B and C). These results suggested that *miR-544a* controlled the location of β-catenin through the regulation of E-cadherin expression.

miR-544a might stabilize β-catenin by the regulation of WNT signaling pathway

Since we found that *miR-544a* regulated the nuclear import of β-catenin, we searched the website, TargetScan Human 6.2 (http://www.targetscan.org/), for direct targets of *miR-544a* related to the WNT signaling pathway. As a result, we focused on *APC2*, *AXIN2* and *GSK-3β* as potential candidates. We first analyzed whether expression of these genes are reduced by overexpression of *miR-544a*. Overexpression of *miR-544a* decreased expression of APC2 and AXIN2, but not GSK3β (Figure 5A). We next performed the luciferase reporter assay using vectors containing the wild type or mutant of each 3′ UTR in these genes. We detected statistically significant reductions in luciferase activity in wild-type constructs, but not in mutant constructs in *AXIN2*, whereas *miR-544a* could not bind to *APC2* (Figure 5B). Furthermore, to investigate whether nuclear imported β-catenin by *miR-544a* induces TCF/LEF activity, we performed TCF/LEF reporter assay with MKN28 cells (Figure 5C). Since TCF/LEF activity was increased by *miR-544a*, expression of *VIM* might

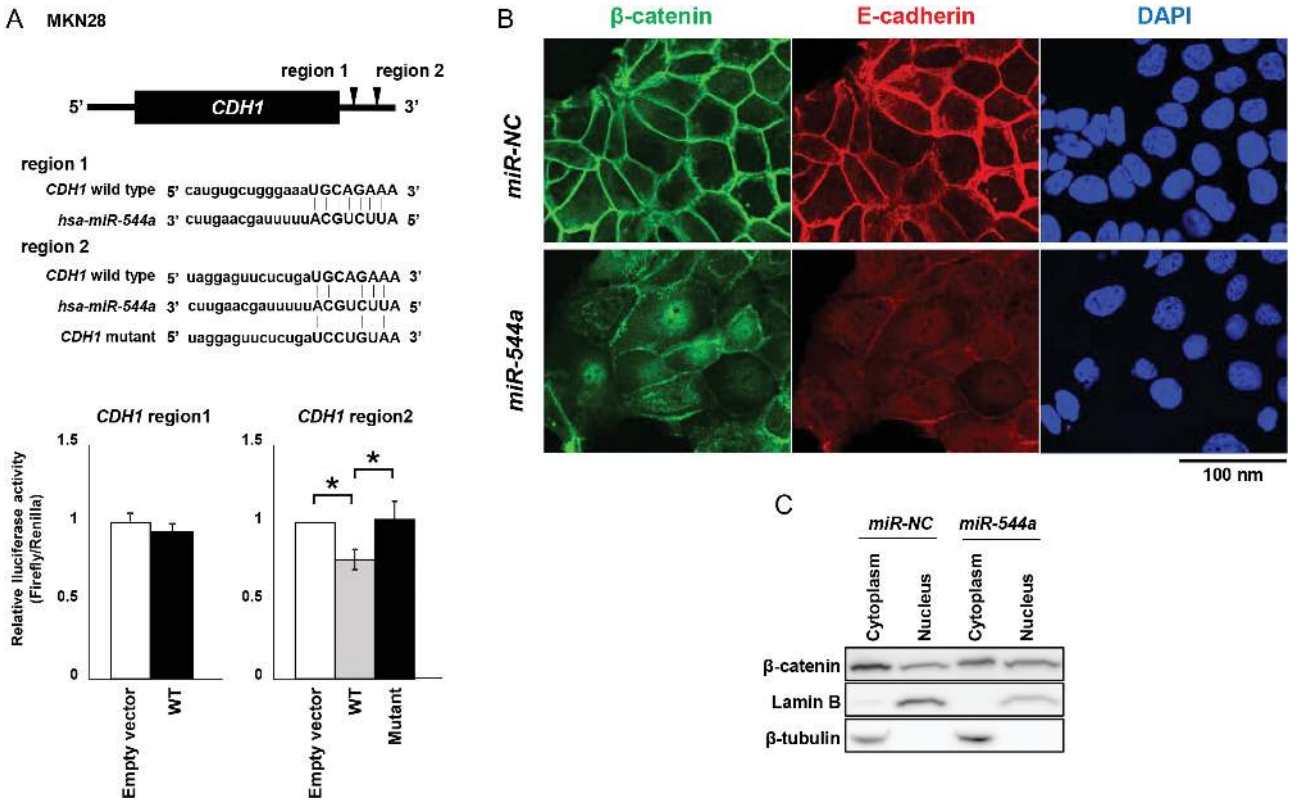

Figure 4. *miR-544a* directly binds to the 3′-UTR region of *CDH1* and induces the nuclear import of β-catenin. (**A**) Confirmation of *CDH1* as a direct target of *miR-544a*. There are two putative binding sites of miR-544a in the 3′-UTR region of *CDH1* (upper). These sites were analyzed using TargetScan Human 6.2. Results of the luciferase reporter assays in MKN1 cells after cotransfection of pMIR-REPORT luciferase vectors containing wildtype (WT) or mutant and *miR-544a* in MKN28 cells are shown (bottom). The Mann–Whitney U-test was used for statistical analysis; asterisks represent $P < 0.05$ versus each control transfectant. (**B**) Immunofluorescent staining of β-catenin (green), E-cadherin (red) and DAPI (blue) in MKN28 cells after transfecting *miR-NC* or *miR-544a*. (**C**) The location of β-catenin was confirmed by western blotting using separately extracted nuclear and cytoplasmic proteins in MKN28 cells. LaminB and β-tubulin are used for loading control of nucleus and cytoplasm, respectively.

be induced through the activation of WNT signaling pathway. Taken together, our findings suggested that *miR-544a* induces the nuclear import of β-catenin and suppresses E-cadherin and AXIN2, resulting in the induction of EMT through the activation of TCF/LEF (Figure 5D).

Discussion

EMT is known to contribute to cancer progression and metastasis (4,6–8). Cancer cells undergoing EMT can acquire invasion capability and enter the surrounding tissue, resulting in the induction of metastasis. Moreover, the effect of EMT not only includes increasing migration, invasion ability and metastatic potential, but also the acquisition of chemoresistance. Taken together, we consider that the development of EMT inhibitors might provide opportunities for both prevention and treatment of cancer. Presently, most anticancer drugs target overexpressed oncogenes in cancer cells, whereas there are very few therapies targeting tumor suppressor genes. Thus, the identification of EMT-inducing miRNAs may be key in leading to the development of other effective anticancer therapeutics.

In this study, we identified *miR-544a* as an EMT-inducing miRNA by function-based screening. Although *miR-544a* induces an EMT phenotype by targeting *CDH1* directly and increases migration and invasion ability (24), the detail mechanisms remain unclear. Moreover, a previous study revealed that the acquisition of the self-renewal ability is induced by activation of the WNT signaling pathway through degradation of GSK3β which is a direct target of *miR-544a* in lung cancer (25). Therefore, we hypothesized that *miR-544a* might induce EMT by the regulation of both the reduction of adhesion molecules and the activation of WNT signaling pathway through targeting genes involved in this pathway. We first revealed that increasing of Snail and ZEB1 expression by *miR-544a* was one of EMT-inducing mechanisms. Moreover, we also confirmed that *CDH1* was directly targeted by *miR-544a* leading to the reduction of E-cadherin. However, a reduction in GSK3β protein with *miR-544a* was not observed, indicating that *GSK3β* is not a target of *miR-544a* in MKN28 cells. An examination of other WNT signal-related genes, *AXIN2* and *APC2*, as candidates target genes showed that *miR-544a* reduced protein levels of these genes; *AXIN2* was a direct target of *miR-544a*, but not *APC2*. Particularly, *AXIN2* is a direct Wnt/β-catenin target gene and functions in a negative feedback loop to control cytosolic β-catenin levels in response to the WNT signaling pathway (26). Thus, reduction of AXIN2 by *miR-544a* might disrupt the function of the WNT signaling pathway. These results suggest that miR-544a suppresses E-cadherin expression and regulates the WNT signaling pathway through the reduction of AXIN2 and APC2 in GC, directly and indirectly.

β-catenin is known to regulate the canonical WNT signaling pathway through its degradation or translocation into the nucleus and maintaining cell–cell adhesion by binding to E-cadherin in cytoplasm (27). It has also been reported that the aberration of β-catenin, inducing the activation of function, was frequently detected in GC and affected the function of the

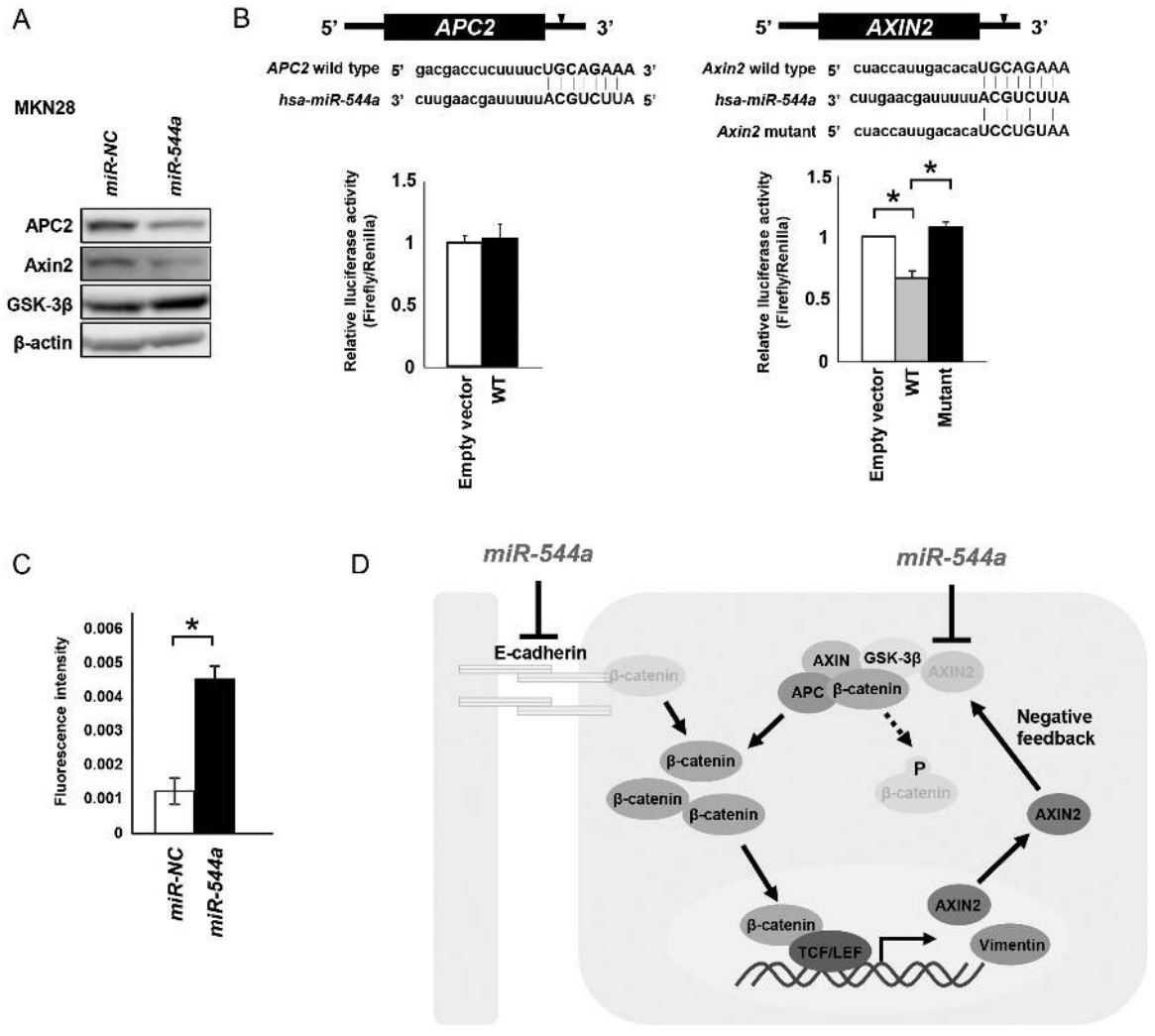

Figure 5. *miR-544a* directly targets both CDH1 and AXIN2 and may activate the WNT signaling pathway. (**A**) APC2, AXIN2 and GSK3β associated with the β-catenin complex are detected by western blotting in MKN28 cells 72 h after transfection of *miR-544a* or *-NC*. (**B**) Schematic of the putative binding site of miR-544a in the 3′-UTR region of *APC2* and *AXIN2*. Results of the luciferase reporter assays in MKN28 cells after cotransfection of the pMIR-REPORT luciferase vectors containing wildtype (WT) of *APC2* and *AXIN2* or mutant of *AXIN2* and *miR-544a* in MKN28 cells. (**C**) TCF/LEF reporter assay was performed with *miR-NC* or *miR-544a* transfectants in MKN28 cells. Experiments were performed in duplicate, and each data point represents the mean (bars, SD). The Mann–Whitney *U*-test was used for statistical analysis; asterisks represent $P < 0.05$ versus each control transfectant. (**D**) Model for *miR-544a*-mediated pathway in EMT.

WNT signaling pathway (28). Moreover, β-catenin in the nucleus forms a complex with TCF/LEF, resulting in the induction of cellular effects involving tumor development and EMT in cancer. Since we found that *miR-544a* reduces expression of E-cadherin, AXIN2 and APC2, we evaluated the nuclear import of β-catenin. As expected, β-catenin was translocated from the cytoplasm to the nucleus by *miR-544a*. In addition, we could confirmed that nuclear imported β-catenin by *miR-544a* induces TCF/LEF activity; in other words, *miR-544a* activated WNT signaling pathway, resulting in the induction of *VIM* expression. Consequently, the mechanism by which EMT is induced by *miR-544a* showed to be a translocation of β-catenin to the nucleus by the reduction of E-cadherin, AXIN2 and APC2 expression.

In conclusion, we established a cell-based reporter system for monitoring the promoter activity of *VIM*, and identified *miR-544a* as an EMT-inducing miRNA using this system. Overexpression of *miR-544a* markedly induced the increasing of vimentin expression and reduction of E-cadherin expression and promoted cell motility and invasion *in vitro* in GC cell lines, clearly indicating that *miR-544a* induces EMT. Furthermore, *AXIN2* and *APC2*, which are cardinal components of the WNT signaling pathway, were characterized as direct and indirect targets of *miR-544a*. Taken together, the reduction of E-cadherin, AXIN2 and APC2 induced the nuclear import of β-catenin, so that EMT was occurred by the increasing of TCF/LEF activity. Our results suggest EMT-inducing *miR-544a*, targeting E-cadherin, AXIN2 and APC2, has a potential to become a prognostic marker and therapeutic target for GC.

Supplementary Material

Supplementary Tables 1 and 2 can be found at http://carcin.oxfordjournals.org/

Funding

Grants-in-Aid for Scientific Research <KAKENHI> for Innovative Areas (22134002, 15H05908), (22134002, 25250019) and (23390077) from Ministry of Education, Culture, Sports, Science and Technology (MEXT), the Tailor-Made Medical Treatment with the BioBank Japan Project (BBJ) and the Practical Research for

Innovative Cancer Control (15Ack0106017h0002) from Japan Agency for Medical Research and Development (AMED), Japan.

Acknowledgement

We thank Ayako Takahashi and Rumi Mori for technical assistance.
Conflict of Interest Statement: None declared.

References

1. Ferlay, J. et al. (2015) Cancer incidence and mortality worldwide: sources, methods and major patterns in GLOBOCAN 2012. Int. J. Cancer, 136, E359–E386.
2. Matsuda, A. et al.; Japan Cancer Surveillance Research Group. (2014) Cancer incidence and incidence rates in Japan in 2008: a study of 25 population-based cancer registries for the Monitoring of Cancer Incidence in Japan (MCIJ) project. Jpn. J. Clin. Oncol., 44, 388–396.
3. Yang, J. et al. (2008) Epithelial-mesenchymal transition: at the crossroads of development and tumor metastasis. Dev. Cell, 14, 818–829.
4. Thiery, J.P. (2002) Epithelial-mesenchymal transitions in tumour progression. Nat. Rev. Cancer, 2, 442–454.
5. Bryant, D.M. et al. (2008) From cells to organs: building polarized tissue. Nat. Rev. Mol. Cell Biol., 9, 887–901.
6. Thiery, J.P. et al. (2009) Epithelial-mesenchymal transitions in development and disease. Cell, 139, 871–890.
7. Tam, W.L. et al. (2013) The epigenetics of epithelial-mesenchymal plasticity in cancer. Nat. Med., 19, 1438–1449.
8. Lamouille, S. et al. (2014) Molecular mechanisms of epithelial-mesenchymal transition. Nat. Rev. Mol. Cell Biol., 15, 178–196.
9. Berx, G. et al. (2009) Involvement of members of the cadherin superfamily in cancer. Cold Spring Harb. Perspect. Biol., 1, a003129.
10. Cullen, B.R. (2004) Transcription and processing of human microRNA precursors. Mol. Cell, 16, 861–865.
11. Bartel, D.P. (2004) MicroRNAs: genomics, biogenesis, mechanism, and function. Cell, 116, 281–297.
12. Lujambio, A. et al. (2012) The microcosmos of cancer. Nature, 482, 347–355.
13. Esquela-Kerscher, A. et al. (2006) Oncomirs - microRNAs with a role in cancer. Nat. Rev. Cancer, 6, 259–269.
14. Kozaki, K. et al. (2012) Tumor-suppressive microRNA silenced by tumor-specific DNA hypermethylation in cancer cells. Cancer Sci., 103, 837–845.
15. Xu, J. et al. (2009) TGF-beta-induced epithelial to mesenchymal transition. Cell Res., 19, 156–172.
16. Harazono, Y. et al. (2013) miR-655 Is an EMT-suppressive microRNA targeting ZEB1 and TGFBR2. PLoS One, 8, e62757.
17. Yamamoto, S. et al. (2014) The impact of miRNA-based molecular diagnostics and treatment of NRF2-stabilized tumors. Mol. Cancer Res., 12, 58–68.
18. Uesugi, A. et al. (2011) The tumor suppressive microRNA miR-218 targets the mTOR component Rictor and inhibits AKT phosphorylation in oral cancer. Cancer Res., 71, 5765–5778.
19. Tsuruta, T. et al. (2011) miR-152 is a tumor suppressor microRNA that is silenced by DNA hypermethylation in endometrial cancer. Cancer Res., 71, 6450–6462.
20. Takada, H. et al. (2005) Screening of DNA copy-number aberrations in gastric cancer cell lines by array-based comparative genomic hybridization. Cancer Sci., 96, 100–110.
21. Imoto, I. et al. (2001) Identification of cIAP1 as a candidate target gene within an amplicon at 11q22 in esophageal squamous cell carcinomas. Cancer Res., 61, 6629–6634.
22. Kozaki, K. et al. (2008) Exploration of tumor-suppressive microRNAs silenced by DNA hypermethylation in oral cancer. Cancer Res., 68, 2094–2105.
23. Rittling, S.R. et al. (1987) Functional analysis and growth factor regulation of the human vimentin promoter. Mol. Cell. Biol., 7, 3908–3915.
24. Mo, X. et al. (2014) miR-544a promotes the invasion of lung cancer cells by targeting cadherina 1 *in vitro*. Onco. Targets. Ther., 7, 895–900.
25. Mo, X.M. et al. (2014) Downregulation of GSK3β by miR-544a to maintain self-renewal ability of lung caner stem cells. Oncol. Lett., 8, 1731–1734.
26. Jho, E.H. et al. (2002) Wnt/beta-catenin/Tcf signaling induces the transcription of Axin2, a negative regulator of the signaling pathway. Mol. Cell. Biol., 22, 1172–1183.
27. Nelson, W.J. et al. (2004) Convergence of Wnt, beta-catenin, and cadherin pathways. Science, 303, 1483–1487.
28. Polakis, P. (2000) Wnt signaling and cancer. Genes Dev., 14, 1837–1851.